

ORIGINAL RESEARCH PAPER

Characterization of ZnO Nanoparticles Pineapple Skin Extract (*Ananas comosus* L.) as Photocatalytic Activity

Lydia Rohmawati^{1*}, Lytha Rizqika Lailia¹, Nugrahani Primary Putri¹, Munasir Nasir¹, Darminto Darminto²

¹ Department of physics, Faculty of Mathematics and Sciences, Universitas Negeri Surabaya, Surabaya, Indonesia

² Department of Physics, Faculty of Science and Data Analytics, Teknologi Sepuluh Nopember, Surabaya, Indonesia

Received: 2023-08-22

Accepted: 2023-11-25

Published: 2024-01-31

ABSTRACT

This research aims to determine the characteristics of ZnO nanoparticles as a photocatalytic agent. Synthesis of ZnO nanoparticles using green synthesis method from pineapple peel extract, whose results were characterized by X-ray Diffraction, Fourier Transform Infra-red, Field Emission-Scanning Electron Microscopy, Transmission Electron Microscopy, Raman spectroscopy, photoluminescence, and a photocatalytic activity assay. This research showed that ZnO nanoparticles had wurtzite phase, alcohol functional groups, and phenol O-H, C=C alkenes, C-O, C-N, and Zn-O. ZnO nanoparticles had a particle size of 20.04 nm, a polyhedral shape, and a band gap energy of 3.28 eV. The Raman active mode $E_2^{(High)}$ at 439.05 cm^{-1} confirmed the formation of pure phase wurtzite. Photoluminescence results indicated that two emission peaks at 392.07 nm and 595.07 nm were associated with defects such as oxygen and zinc vacancies. This study showed that ZnO nanoparticles were effective in photodegrading methylene blue dye within 180 minutes under UV light irradiation, with a known degradation value reaching 99.86%. In addition, ZnO nanoparticles as a catalyst are very stable and can be reused after five cycles. Thus, the synthesized ZnO nanoparticles can be applied effectively for environmental applications, namely as a photocatalyst in processing textile industry waste, especially for organic dye waste.

Keywords: Zno Nanoparticles, Green Synthesis, Photocatalytic, Pineapple Peel Extract.

How to cite this article

Rohmawati L., Lailia L. R., Putri N. P., Nasir M., Darminto D., Characterization of ZnO Nanoparticles Pineapple Skin Extract (*Ananas comosus* L.) as Photocatalytic Activity. J. Water Environ. Nanotechnol., 2024; 9(1): 112-123. DOI: 10.22090/jwent.2024.01.08

INTRODUCTION

Over the last two years, industrial developments have created chemical wastes polluting water and the surrounding environment. Pollution is known to cause high toxicity [1]. Chemical waste contains toxic dyes and is very dangerous, made from azo compounds and their derivatives, as well as the benzene groups, such as methylene blue [2]. Methylene blue is carcinogenic and can be a source of disease if it is in the environment for a long time [3]. Organic dyes are synthetic materials that the environment cannot degrade so these compounds

can accumulate in nature [4]. With the existence of chemical waste, which is an environmental issue, a method is needed to develop water purification technology that is implemented in different ways, for example, purifier, distillation, adsorption, flocculation, and photocatalyst [5]. Photocatalyst is a possible waste treatment method because the process is simple and effective in cleaning biological and chemical contaminants [6,7].

Moreover, organic photoactive compounds in this photocatalytic process can degrade organic pollutants where the dissolved organic material can function self-cleaning on contaminated surfaces

* Corresponding Authors Email: lydiarohmawati@unesa.ac.id



This work is licensed under the Creative Commons Attribution 4.0 International License.

To view a copy of this license, visit <http://creativecommons.org/licenses/by/4.0/>.

through photodegradation of species that are active when exposed to sunlight [8]. Photocatalytic degradation, which belongs to the advanced oxidation process, is an energy-saving process for degradation processes, where nanostructured photocatalysts play an essential role in promoting accelerated decomposition by generating reactive species such as hydroxyl radical ($\bullet\text{OH}$) and superoxide ($\bullet\text{O}_2^-$) using suitable light and energy [9]. Besides that, the photodegradation of organic dyes can increase due to the presence of hole scavengers [10].

Photocatalytic materials with good photodegradation potential are semiconductors. One of the catalysts used is the semiconductor ZnO (zinc oxide), which has an energy gap ranging from 3.32 to 3.37 eV with a nanostructure so that it can be applied mainly for wastewater treatment. The material has a high redox capability, resulting in considerable electron mobility and better catalytic performance [11]. This semiconductor can produce active substances for photocatalytic applications after irradiating at a specific wavelength [12,13]. ZnO photocatalyst has versatile properties, easy synthesis, and a relatively low cost [14]. In addition, ZnO in powder form also has unique properties, namely being non-toxic, biocompatible, and having high catalytic activity in degrading toxic pollutants [15]. Parvizi et al. (2019) reported that photocatalytic activity is closely related to optical absorption [16]. Among different semiconductors, ZnO nanoparticles have shown higher efficiency in the photocatalytic degradation of some organic dyes than TiO_2 [17]. That is because the number of photogenerated electron-hole recombinations decreases [18]. The catalytic activity of ZnO can be maintained, is stable, and does not experience a significant decrease when reused [19].

ZnO nanoparticles can be extracted from several plants, including pineapple peel extract. Pineapple peel contains bioactive compounds such as saponins, flavonoids, tannins, anthocyanins, vitamin C, carotenoids, and the enzyme bromelain [20]. Mirgane et al. (2020) reported that ZnO nanoparticles from pineapple peel could be used for wastewater treatment [21]. The study showed that 99.60% of the dyestuffs degraded from textile industry wastewater within 900 minutes. In this study, the characteristics of optical properties such as photoluminescence were not reported, even though this photoluminescence technique

can be used to determine the characteristics of photogenerated recombination of electron and hole pairs. Dewi and Rohmawati (2022) reported that ZnO nanoparticles with the wurtzite phase were successfully extracted from pineapple skin, where the manufacturing method used green synthesis [22]. Biosynthesis of ZnO nanoparticles is more provident and environmentally affable than chemical or physical synthesis methods [23].

Based on the information from the research result above, the application of ZnO from pineapple peel extract has never been reported for the degradation of methylene blue so this research will discuss in more detail the characteristics of ZnO nanoparticles from pineapple peel extract as photocatalysts. Apart from that, this research also discusses catalyst stability and the reuse of ZnO nanoparticle catalysts in the degradation of methylene blue dye. The results of this study will provide solutions to the textile industrial waste problem by using natural materials for effective photocatalytic degradation, especially for organic dye waste.

MATERIAL AND METHODS

Materials

The tools and materials used were pineapple skin (*Ananas comosus* L.), distilled water, zinc acetate dihydrate (Merck), NaOH 1M (Merck), methylene blue (Merck), mortar pestle, spatula, digital balance, oven, beaker, centrifuge, stirrer, sonicator, measuring cup, petri dish, funnel, pH paper, filter paper Whatman, and aluminum foil.

Green synthesis of ZnO nanoparticles

The synthesis of ZnO nanoparticles was done by peeling the pineapple fruit, taking the inner skin pericarp, and then rinsing it with distilled water. As much as 10 grams of pineapple peel were mashed using a mortar pestle, then the results were put into a 250 mL beaker, and 100 mL of distilled water was added. The solution was stirred at 300 rpm at 75°C for 1 hour. After that, the solution was filtered, and a yellow filtrate was obtained. The result is added 10 mL of distilled water and 4 grams of zinc acetate dihydrate, then sonicated at 40°C for 1 hour. Furthermore, 100 mL of 1 M NaOH was added to mold a milky white solution, then centrifuged at 3000 rpm, and the results were parched at 120°C for 12 hours. Here is a chemical reaction during green synthesis using NaOH solution.

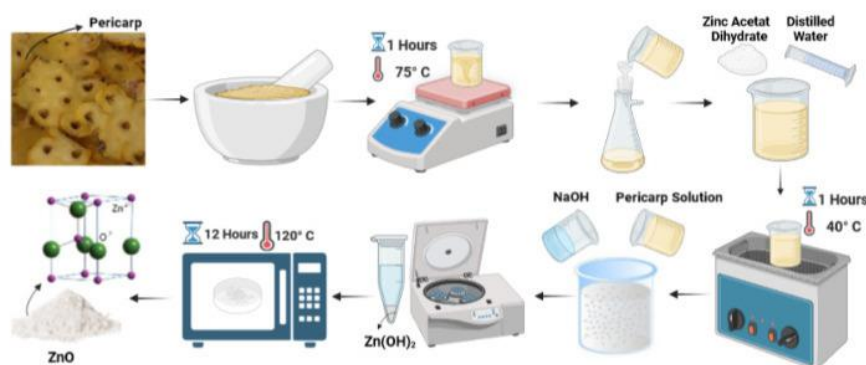
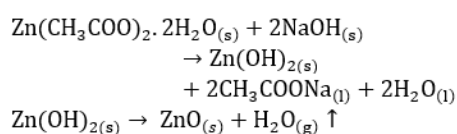


Fig 1. Green synthesis of ZnO nanoparticles



Characterization of ZnO nanoparticles

XRD (X-ray Diffraction) characterization was used to determine the formation of the primary phase in the ZnO sample. The type of XRD tool used was Smartlab Rigaku with a Cu anode radiation source, 40 kV, 30 mA, 0.01°/minute with a CuK α wavelength of 1.54056 Å and an angle (2 θ) of 5°-90°. The phases contained in the sample could be identified through qualitative analysis using the software Match!. FTIR characterization (Fourier Transform Infrared Spectroscopy) type Thermoscientific Nicolet Is-10 was used to identify groups of chemical bonds owned by the test sample with absorption peaks at wave numbers 4000-500 cm⁻¹. The morphology of the sample in the form of the synthesized grain shape could be identified using the FE-SEM tool (Field Emission-Scanning Electron Microscopy) at 20000 times magnification with the type Jeol JSM-IT200 equipped with EDX (Energy Dispersive X-Ray). The synthesized nanoparticles' shape, structure, and distribution could be known from the TEM characterization results (Transmission Electron Microscopy) of the Hitachi H7700, where the analytical method used ImageJ software. The typical vibration mode of the material could be identified using the Raman spectroscopy characterization tool iHR320 HORIBA and a laser source with a wavelength of 532 nm. The interaction between the monochromatic light radiation source and the sample caused scattering due to the vibration of the

identified compounds. The results of the Raman Spectroscopy test were in the form of a relationship graph between intensity and wavenumber. The sample vibration peaks were identified at wave numbers 2000-265 cm⁻¹. With a 325 nm laser beam and a 1200 g/mm grating, a Horiba Scientific PL (Photoluminescence Microspectrometer) was used to identify structural defects in materials such as oxygen vacancies. The data from the test was in the form of a relationship graph intensity, and the wavelength (nm) ranges from 300-600 nm, which was then plotted using the graph software Origin 8.0; then, the results were matched with data from the journal references. The UV-Vis characterization of the Hitachi UH-5300 spectrophotometer was used to measure the absorbance of a sample with a wavelength of 200-800 nm. Based on the data from this characterization, the band gap analysis could be done using the Tauc plot analysis.

Photocatalytic Activity

Before adding the ZnO nanoparticle powder catalyst to the Methylene Blue (MB) solution, it is necessary to make a 30 ppm MB solution first, namely, 30 ml of MB solution (100 ppm) mixed with 100 ml of distilled water, then stir until evenly mixed. After that, 10 mg of ZnO nanoparticle powder was added to the solution and stirred using a magnetic stirrer for 30 minutes at 300 rpm. After that, it was irradiated using a UV Sterilizer lamp (10 W with 30 mW/cm²) with time intervals of 30, 60, 90, 120, 150, and 180 minutes. The solution resulting from the irradiation was centrifuged for 15 minutes at a speed of 3000 rpm so that it was homogeneous and no lumps of catalyst were found in the solution. After that, the

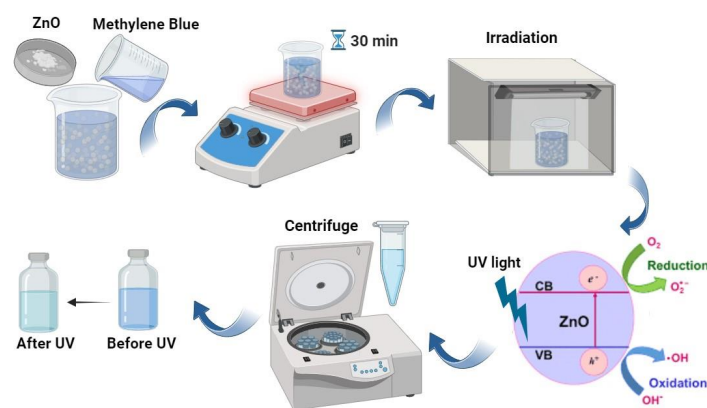


Fig 2. Photocatalyst activity

solution was put into a glass vial (10 ml) for UV-vis characterization.

The solution MB absorbance value, degraded with a catalyst, was measured using a UV-Vis spectrophotometer. The test results were plotted using the graphing software Origin 8.0 to obtain the curve for the linear regression equation.

$$\% \text{ Degradation} = \frac{C_0 - C_t}{C_0} \times 100 \%$$

% Degradation is the percentage of degradation, C_0 is the initial concentration of methylene blue without irradiation, and C_t is the final concentration of methylene blue at time t after the photocatalytic process [24].

RESULT AND DISCUSSION

XRD Characterization Results

The diffraction pattern of the synthesized sample can be seen in Fig. 3, which is then analyzed using the software Match!. The synthesized sample has a phase wurtzite formed at an angle of 2θ of 36.253° . At this angle, it has the highest diffraction intensity with crystal orientation (101), following JCPDS card number 01-079-0206, and following the research results of Ahmad et al. (2019) and Sari et al. (2021), namely at an angle of 36.245° [25] and 36.28° [26]. Other diffraction peaks indicate phase wurtzite at angles of 31.768° , 34.422° , 36.253° , 47.539° , 56.594° , 62.858° , 66.374° , 67.947° , 69.085° , 72.568° , 76.959° , 81.387° and 89.613° with miller indices (100), (002), (101), (102), (110), (103), (200), (112), (201), (004), (202), (104), and (203). The diffraction pattern of Fig. 3 is also not found in impurity, so it can be said that all of the synthesized samples are the wurtzite phase of ZnO.

FTIR Characterization Results

The functional groups of the synthesized ZnO nanoparticles were identified in the FTIR spectra with wave numbers of $4000-500 \text{ cm}^{-1}$ (Fig. 4). The absorption peak at wave number 3350 cm^{-1} showed the presence of alcohol and phenol O-H bonds, and this was following the results of Nagajyoti et al. (2015) which were at wave number 3380 cm^{-1} [27]. The alkene chemical bond C=C was detected at a wave number of 1653 cm^{-1} . Bond vibrations of C=O with carboxylic acid groups were indicated at wave number 1549 cm^{-1} .

In addition, at 1438 cm^{-1} denotes the C-O functional group, and at 1082 cm^{-1} , a C-N vibration occurs. At the absorption peak of 866 cm^{-1} , the conformation of Zn tetrahedral coordination occurs, following the results by Jurablu et al. (2015), which were at wave number 875 cm^{-1} [28]. Functional groups of Zn-O are found at wave numbers 782, 688, and 548 cm^{-1} . Basri et al. (2020) reported in their research that the functional groups of ZnO nanoparticles were at wave numbers of $800-400 \text{ cm}^{-1}$ [29]. Detailed information about the absorption peaks in the samples can be seen in Table 1.

Table 1. Identification of the functional groups of the samples

Wavenumber (cm^{-1})		Bond type
Experiment	Reference	
3350	3380 [22]	O-H
1653	1660 [30]	-C=C
1549	1562-1577 [31]	C=O
1438	1425-1446 [31]	C-O
1082	1075 [30]	C-N
866	875 [28]	Zn
782, 688, 548	443, 546 [32]	Zn-O

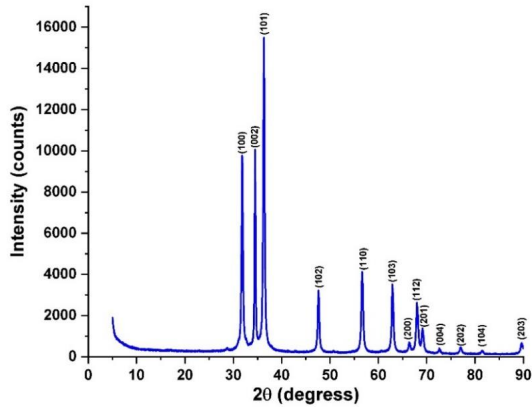


Fig 3. The diffraction pattern of the synthesized sample

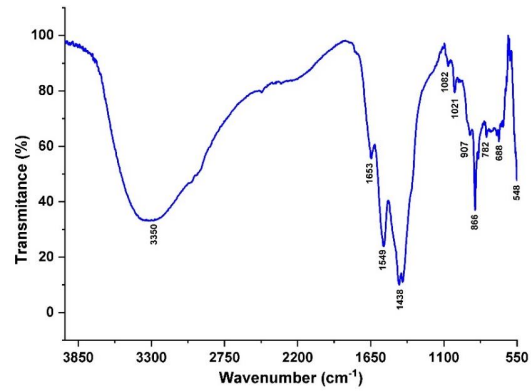
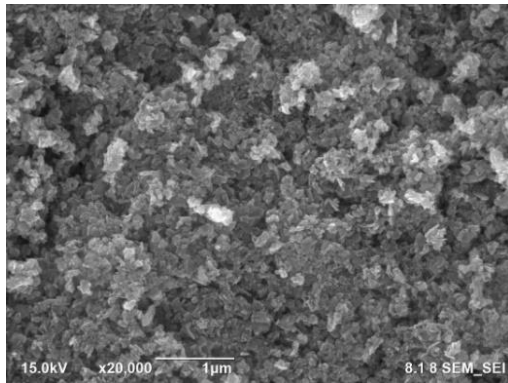
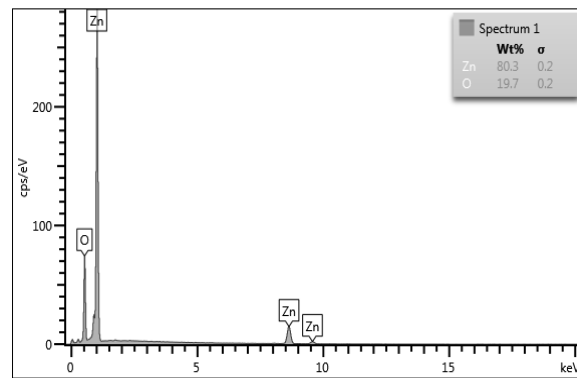


Fig 4. FTIR spectra of the synthesized sample



(a)



(b)

Fig 5. Characterization results of samples synthesized using (a) FE-SEM and (b) EDX

FE-SEM Characterization Results

The morphology of the synthesized ZnO nanoparticles was determined by FE-SEM analysis at 20,000x magnification, as shown in Fig. 5. FE-SEM shows that the synthesized samples have a polyhedral shape with a uniform size distribution, although the sample dimensions cause some agglomeration. The content and percentage by weight of elements can be known from the results of the EDX spectrum, where peaks appear corresponding to the ZnO content, namely the presence of O and Zn elements with percentages of 19.7% and 80.3%, respectively. On the contrary, this EDX analysis demonstrated the purity of the synthesized ZnO nanoparticles, which comprise a high composition of Zn and O elements [33].

TEM Characterization Results

Particle size distribution can be known using ImageJ, namely by considering 100 items per sample. Fig. 6 shows that the synthesized

samples have a uniform polyhedral shape, low agglomeration, and an average particle size of 20.04 nm. Based on the particle size, the synthesized ZnO sample can be said to be a nanoparticle because the grain size is less than 100 nm. A regular and uniform polyhedral surface can be associated with the increased photocatalytic ability of ZnO nanoparticles [34].

Raman Spectroscopy Characterization Results

Data from spectroscopic Raman characterization results are shown in Fig. 7. Raman from ZnO nanoparticles with structure wurtzite pertains to the space group C_{6v}^4 ($P6_3mc$), generating a vibrational pattern in the Brillouin zone [35].

$$A_1 + 2B_1 + E_1 + 2E_2$$

Known $2B_1$ is a stationary phonon, while the other mode is a Raman active phonon [35]. Mode A_1 and E_1 are polar modes divided into optical transverse (TO) and optical longitudinal (LO).

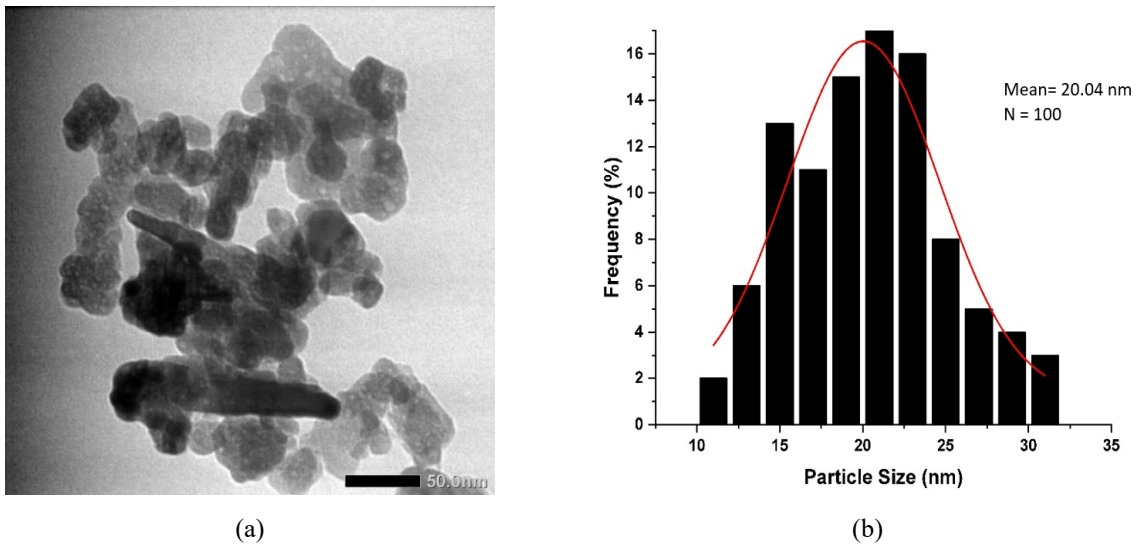


Fig 6. (a) TEM micrograph, (b) Particle size distribution of the synthesized ZnO nanoparticles

Table 2. Raman spectrum of ZnO nanoparticles

Raman shift (cm ⁻¹)		Symmetry process
Experiment	Reference	
100.26	99 [38]	E ₂ ^(Low)
203.532	203 [38]	2E ₂ ^(Low)
335.04	333 [38]	E ₂ ^(High) - E ₂ ^(Low)
439.05	440 [37]	E ₂ ^(High)
582.65	576 [38]	A ₁ (LO)
618.997	587 [38]	E ₁ (LO)
653.82	667.82 [40]	TA + LO
928.09	984 [41]	A ₁ (LO) + E ₂ ^(High)
1080.62	1079 [38]	TO + LO
1346.16	1158 [38]	2A ₁ (LO)
1418.34	1550 [38]	2E ₁ (LO)

Mode E₂ is a non-polar mode consisting of E₂^(low) and E₂^(high) phonons. Mode E₂^(low) is a vibrational mode of the zinc lattice, and mode E₂^(high) is an arrangement of wurtzite, a ZnO nanoparticle lattice that includes shifts of oxygen atoms [36]. Mode E₂^(Low) at 100.26 cm⁻¹ and mode E₂^(High) at 439.05 cm⁻¹ are characteristic phonons of wurtzite-phase ZnO nanoparticles that have good crystallinity in the ZnO structure and are related to the vibration of zinc oxygen in the crystal lattice [37]. Mode LO is at 232.85 cm⁻¹ A₁ and 618.997 cm⁻¹ E₁. Mode A₁ (LO) and E₁ (LO) are associated with interstitial oxygen or zinc vacancies. At 203.536 cm⁻¹, 2E₂^(Low) is an overtone of E₂^(Low), and another at 335.04 cm⁻¹ E₂^(Low) -

E₂^(High), a combination of E₂^(Low) and E₂^(High) [38].

The Raman spectrum also shows broad peaks ranging from 653.82, 1346.16, and 1418.34 cm⁻¹, which belong to the multiphonon process due to the combination of optics. A mode vibrational activity A₁ (LO) + E₂^(High) at 928.09 cm⁻¹ is a multiphoton scattering mode. The vibration mode is detected at 582.65 cm⁻¹ of which E₁ (LO) is activated; this mode indicates the process of multiphonon resonance in the ZnO nanoparticle structure. Optical phonon activation is associated with interstitial oxygen defect formation in Zn [39]. For a more detailed explanation, it can be seen in Table 2 regarding the summit of the Raman spectrum on the synthesized samples.

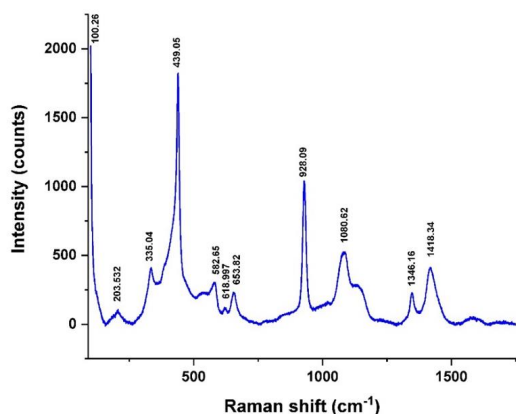


Fig 7. Raman spectrum of the synthesized samples

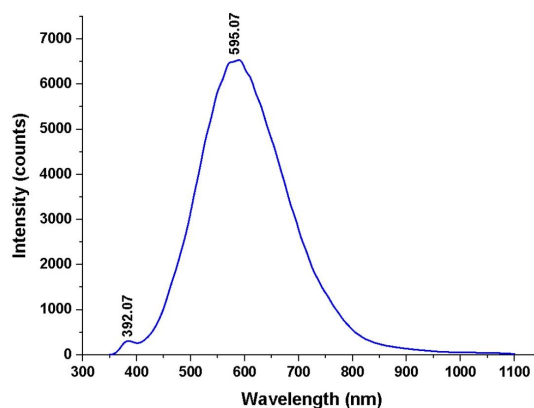


Fig 8. Photoluminescence of synthesized ZnO nanoparticles

PL Characterization Results

Photoluminescence (PL) of ZnO nanoparticles was performed to come across structural imperfection primarily owing to Zn and oxygen vacancies. Fig. 8 shows that synthesized samples' PL exhibits two emission peaks, such as emission peak at 392.07 nm is related to Near Band Emission (NBE) [42], and the emission peak is located at 595.07 nm and is related to Deep Level Emission (DLE) namely oxygen and Zn vacancies. The UV emission band, known as the NBE band gap of ZnO nanoparticles, is caused by the excitonic recombination of holes in the valence band and electrons in the conduction band through the exciton collision process.

Meanwhile, visible light emission, known as DLE, is caused by crystal defects [43]. DLE can be attributed to the recombination of electrons and holes at the deep band gap level caused by the presence of various crystal defects in the lattice of ZnO nanoparticles such as zinc interstitial (Zn_i), zinc vacancies (V_{Zn}), oxygen vacancies (V_O), interstitial oxygen (O_i), and oxygen antisite (O_{Zn}). The vacancies of Zn, oxygen, and interstitial atoms in the synthesized samples can be observed through PL measurements and Raman spectroscopy. Various types of defects, specifically V_O (oxygen vacancies), are known to exist in three configurations such as neutral oxygen vacancies (V_O), single ionized oxygen vacancy (V_O^+), and double ionized oxygen vacancy (V_O^{2+}). Based on the emission spectrum in Fig. 8, it is appreciated that the presence of oxygen vacancies can increase photocatalytic activity. It is related to the oxygen vacancy in the sample, which will cause the positive free charge (hole) to attract oxygen more quickly

and form H_2O_2 , producing hydroxyl radicals.

Photocatalytic ZnO Nanoparticles

The photocatalytic performance of ZnO nanoparticles is highly dependent on their electronic band structure and bandgap energy. The results of the UV-vis characterization using the Tauc plot analysis are in Fig. 9. It is known that the synthesized ZnO nanoparticles have an energy gap of around 3.28 eV; this is smaller than 3.37 eV, which is the standard ZnO energy gap. This means that the photocatalyst activity of the ZnO nanoparticles is efficient because the generated electrons are more easily excited and produce more hydroxyl radicals. This hydroxyl radical is used as an oxidizer for methylene blue (MB) compounds to become harmless substances. The absorption peak of ZnO nanoparticles was found at a wavelength of 380 nm in the UV region; this result follows the study by Alharshan et al. [44].

The UV-vis absorption spectrum of ZnO nanoparticles towards MB dye with varying times during the photodegradation process up to 180 minutes is shown in Fig. 10. There was a difference in the uptake of methylene blue dye (control) in the presence of ZnO nanoparticle catalyst without UV light irradiation, where the uptake of methylene blue dye decreased from 2.217 to 0.625 a.u. The absorption intensity of MB dye gradually decreases with the length of time of UV irradiation, especially at a wavelength of 664 nm, which is indicated by the fading of the dye MB until it becomes clear, which indicates degradation of the MB dye molecules. That is because the longer the radiation exposure time, the color of the solution will fade, making it easier to reach the photocatalyst. It is

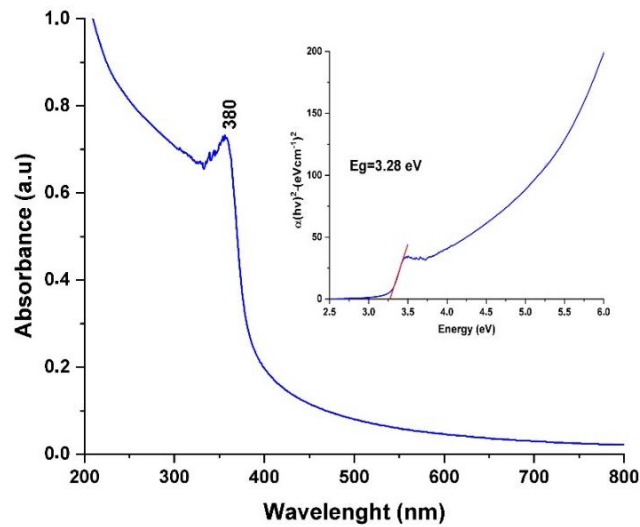


Fig 9. UV-vis absorption spectrum and band gap in ZnO nanoparticles

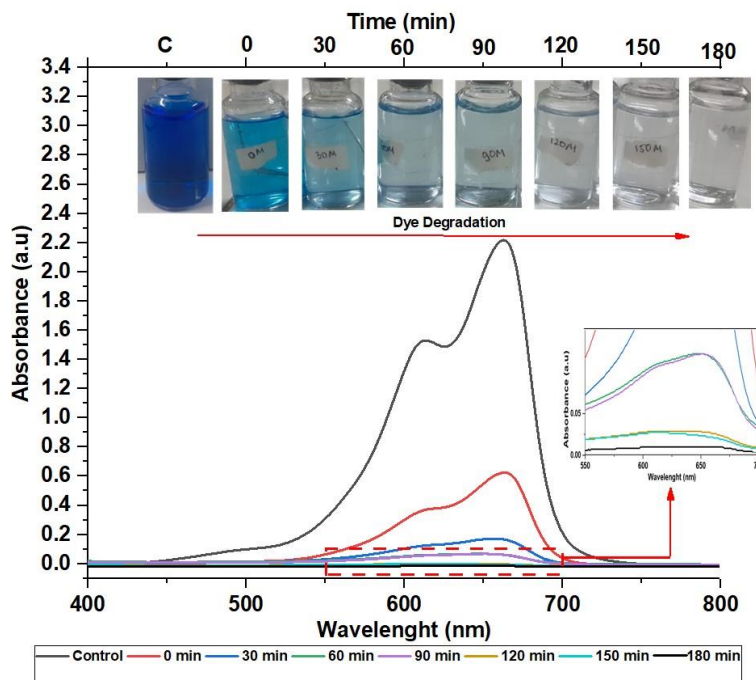


Fig 10. UV-vis absorption spectrum of ZnO nanoparticles against MB dye

known that the degradation of MB solution dye without UV irradiation is 71.81%. When exposed to UV irradiation for 30, 60, 90, 120, 150, and 180 minutes, the MB dye was degraded with percentages of 92.47, 97.20, 97.25, 99.32, 99.68 and 99.86%, respectively (Fig. 11).

The duration of irradiation can affect the degradation percentage of methylene blue by a photocatalyst (Fig. 11). This is due to the

interaction between the dye molecules and the photocatalyst surface. The longer the irradiation time, the more dyes can be degraded until they reach their optimum time because of the large number of \bullet OH radicals formed. The duration of irradiation indicates the interaction between the photocatalyst and UV light to produce \bullet OH radicals and the interaction between \bullet OH radicals and methylene blue dyes. The OH radical plays a

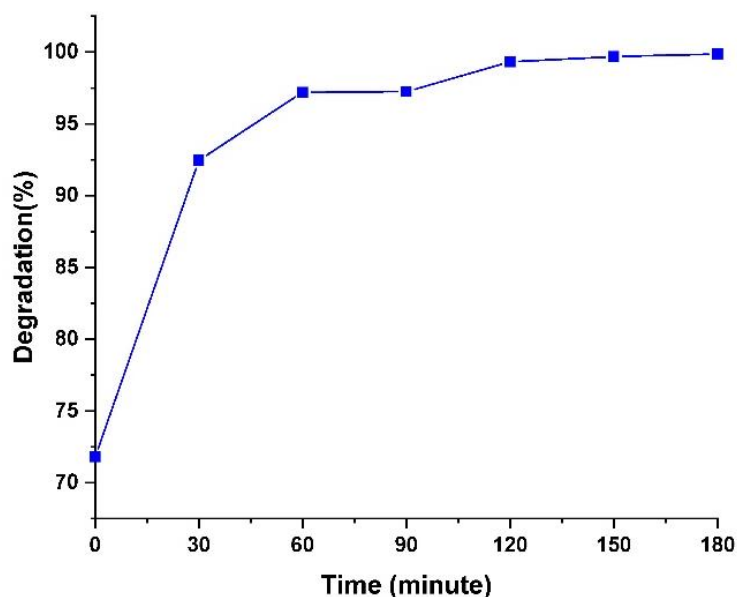


Fig 11. The effect of irradiation time on the degradation of MB dyes

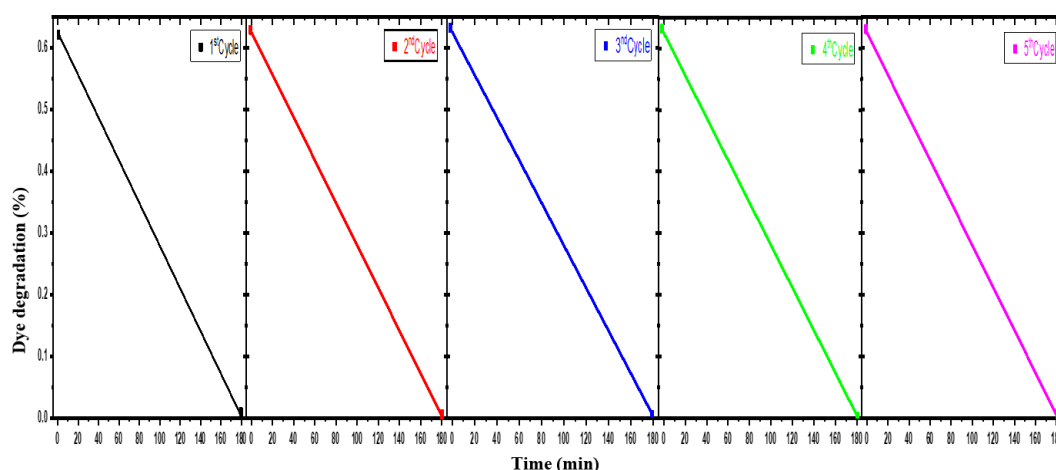


Fig 12. Stability test and reuse of ZnO nanoparticles catalyst

role in the decomposition of methylene blue to be a safe compound, so the longer the irradiation time, the more $\bullet\text{OH}$ radicals are formed and the greater the percent degradation value produced. With an increase in the photon energy produced, more $\bullet\text{OH}$ is produced and formed. It is a potent oxidizing agent that can be used to degrade MB dyes [45].

In this research, ZnO nanoparticles synthesized using the green synthesis method showed good photocatalytic performance, especially in degrading MB dye under UV light irradiation, which is known to have the highest degradation efficiency of 99.86% in a short time, 180 minutes. Several studies on the photodegradation activity

of MB with ZnO nanoparticles using several methods are shown in Table 3. Based on the results of several researchers, all previously reported that ZnO nanoparticle photocatalysts required a longer reaction time to degrade the dye, and the degradation rate was relatively low. Thus, the ZnO nanoparticles synthesized in this study showed excellent photocatalytic activity with increasing irradiation time. The ZnO nanoparticle catalyst degraded the MB dye, and the MB dye solution was almost completely degraded.

Catalyst stability and catalyst reuse were carried out using five experimental cycles, namely using UV irradiation for 180 minutes, the results of

Table 3. Results of photocatalytic degradation of MB dyes

Method	ppm MB	Degradation (%)	Time (min)	References
Green synthesis	20	74.15	160	[46]
Green synthesis	25	88.39	180	[45]
Green synthesis	30	99.86	180	This work

which are shown in Fig. 12. ZnO nanoparticles as a catalyst remained active against UV light, and the absorption of MB dye remained stable with a degradation value of 99.86%. It confirms that the synthesized ZnO nanoparticles can be applied effectively for environmental applications, namely as a photocatalyst in textile industry waste processing.

CONCLUSION

ZnO nanoparticles were successfully synthesized using the method of green synthesis and have a phase wurtzite, polyhedral shape with an average particle size of 20.04 nm, have alcohol and phenol O-H functional groups, C=C alkene, C-O, C-N, and Zn-O. In addition, ZnO nanoparticles have a Raman active optical phonon mode $E_2^{(High)}$ at 439.05 cm^{-1} , which confirms the formation of the phase wurtzite. The photoluminescence characterization showed two emission peaks at 392.07 nm and 595.07 nm. These two peaks are associated with structural defects such as oxygen vacancies and Zn. ZnO nanoparticles have an energy gap of 3.28 nm with an absorption peak at a wavelength of 380 nm, which is in the UV region. The results of the photocatalytic effectiveness test showed that the percent degradation value of ZnO nanoparticles from pineapple peel extract with a catalyst mass of 10 mg and 30 ppm methylene blue is capable of degrading dyes by 99.86% within 180 minutes. Thus, the longer the irradiation time, the higher the percent degradation value of methylene blue, such as organic dyes. ZnO nanoparticles as a catalyst have stability in absorbing methylene blue dye and remain active under UV light even though the ZnO nanoparticle catalyst has been reused after five cycles. Thus, ZnO nanoparticles from pineapple peel are effective as photocatalytics and can be applied in processing organic dye waste.

ACKNOWLEDGEMENT

The author would like to thank the Physics Laboratory and Integrated Laboratory of Universitas Negeri Surabaya, Central Laboratory

Physics Research of the National Research and Innovation Agency (BRIN), University of Indonesia Chromatography Laboratory (UI), and Gajah Mada University Inorganic Chemistry Laboratory (UGM) for the support of laboratory.

CONFLICT OF INTEREST

The authors declare no conflict of interest.

REFERENCES

- [1] J. Singh, S. Kumar, Rishikesh, A. K. Manna, R. K. Soni, "Fabrication of ZnO-TiO₂ Nanohybrids for Rapid Sunlight Driven Photodegradation of Textile Dyes and Antibiotic Residue Molecules", *Optical Materials*, vol. 107, pp. 1-12, Sept 2020. <https://doi.org/10.1016/j.optmat.2020.110138>
- [2] R. Putri, H. Sanjaya, "Degradasi Zat Warna Methanil Yellow Menggunakan Metoda Fotosonolisis dengan Bantuan Katalis ZnO", *Periodic*, vol. 11, no. 1, pp. 98-101, 2022. <https://doi.org/10.24036/p.v11i1.113422>
- [3] A. Phuruangrat, B. Kuntalue, S. Thongtem, T. Thongtem, "Hydrothermal Synthesis of Hexagonal ZnO Nanoplates Used for Photodegradation of Methylene Blue", *Optik*, vol. 226, no. 1, pp. 1-7, Jan 2021. <https://doi.org/10.1016/j.ijleo.2020.165949>
- [4] N. Barbero, D. Vione, "Why Dyes Should Not Be Used to Test the Photocatalytic Activity of Semiconductor Oxides", *Environmental Science and Technology*, vol. 50, no. 5, Feb 2016. <https://doi.org/10.1021/acs.est.6b00213>
- [5] R. Sabouni, H. Gomaa, "Photocatalytic Degradation of Pharmaceutical Micro-Pollutants using ZnO", *Environmental Science and Pollution Research*, vol. 26, pp. 5372-5380, Jan 2019. <https://doi.org/10.1007/s11356-018-4051-2>
- [6] D. Tekin, H. Kiziltas, H. Ungan, "Kinetic Evaluation of ZnO/TiO₂ Thin Film Photocatalyst in Photocatalytic Degradation of Orange G", *Journal of Molecular Liquids*, vol. 306, pp. 1-6, May 2022. <https://doi.org/10.1016/j.molliq.2020.112905>
- [7] L. Munguti, F. Dejene, "Influence of Annealing Temperature on Structural, Optical and Photocatalytic Properties of ZnO-TiO₂ Composites for Application in Dye Removal in Water", *Nano-Structures & Nano-Objects*, vol. 24, pp. 1-16, Oct 2020. <https://doi.org/10.1016/j.nanoso.2020.100594>
- [8] R. M. Kakhki, R. Tayebee, S. Hedayat, "Phthalhydrazide nanoparticles as new highly reusable organic photocatalyst in the photodegradation of organic and inorganic contaminants", *Applied Organometallic Chemistry*, vol. 32, no. 2, pp. 1-9, 2017. <https://doi.org/10.1002/aoc.4033>
- [9] S. S. Ali, I. A. Qazi, M. Arshad, Z. Khan, T. C. Voice, C. T. Mehmood, "Photocatalytic Degradation of Low Density Polyethylene (LDPE) Films using Titania

- Nanotubes”, Environmental Nanotechnology, Monitoring & Management, vol. 5, pp. 44-53, May 2016. <https://doi.org/10.1016/j.enmm.2016.01.001>
- [10] R. Tayebee, R. M. Kakhki, P. Audebert, M. M. Amini, M. Salehi, N. M. Ghohe, V. Mandanipour, G. R. Karimipour, “A robust UV-visible light driven SBA 15 PS/phthalhydrazide nanohybrid material with enhanced photocatalytic activity in the photodegradation of methyl orange”, Applied Organometallic Chemistry, vol. 32, no. 7, pp. 1-11, Feb 2018. <https://doi.org/10.1002/aoc.4391>
- [11] T. S. Tofa, K. L. Kunjali, S. Paul, J. Dutta, “Light Photocatalytic Degradation of Microplastic Residues with Zinc Oxide Nanorods”, Environmental Chemistry Letters, vol. 17, pp. 1341-1346, 2019. <https://doi.org/10.1007/s10311-019-00859-z>
- [12] H. Kamani, S. Nasser, M. Khoobi, R. N. Nodehi, A. H. Mahvi, “Sonocatalytic Degradation of Humic Acid by N-Doped TiO₂ Nano-Particle in Aqueous Solution”, Journal of Environmental Health Science and Engineering, vol. 14, no. 1, pp. 1-9, Dec 2016. <https://doi.org/10.1186/s40201-016-0242-2>
- [13] R. Ashouri, P. Ghasemipour, B. Rasekh, F. Yazdian, S. R. Mofradnia, M. Fattahi, “The Effect of ZnO-Based Carbonaceous Materials for Degradation of Benzoic Pollutants: A Review”, International Journal of Environmental Science and Technology, vol. 16, no. 13, pp. 1729-1740, Oct 2018. <https://doi.org/10.1007/s13762-018-2056-5>
- [14] R. Yulina, S. Gustiani, W. Septiani, “Pembuatan dan Karakterisasi Serat Hollow dari Selulosa Bakterial dengan Nanopartikel ZnO untuk Pengolahan Air Limbah Tekstil”, Arena Tekstil, vol. 29, no. 1, pp. 47-54, 2014. <https://doi.org/10.31266/at.v29i1.849>
- [15] R. M. Kakhki, R. Tayebee, F. Ahsani, “New and highly efficient Ag doped ZnO visible nano photocatalyst for removing of methylene blue”, Journal of Materials Science: Materials in Electronics, vol. 28, pp. 5941-5952, Jan 2017. <https://doi.org/10.1007/s10854-016-6268-5>
- [16] E. Parvizi, R. Tayebee, E. Koushki, M. F. Abdizadeh, B. Maleki, P. Audebert, L. Galmiche, “Photocatalytic efficacy of supported tetrazine on MgZnO nanoparticles for the heterogeneous photodegradation of methylene blue and ciprofloxacin”, RSC Advances, vol. 9, pp. 23818-23831, 2019. <https://doi.org/10.1039/c9ra04702f>
- [17] F. Khan, S. A. A. Ansari, A. Ahmad, “Study of Photocatalytic activity of ZnO and TiO₂ nanoparticles”, International Journal of Engineering and Applied Sciences, vol. 4, no. 11, pp. 130-136, Nov 2017.
- [18] R. Tayebee, E. Esmaeili, B. Maleki, A. Khoshniat, M. Chahkandi, N. Mollania, “Photodegradation of methylene blue and some emerging pharmaceutical micropollutants with an aqueous suspension of WZnO-NH₂@H3PW12O₄₀ nanocomposite”, Journal of Molecular Liquids, vol. 317, pp. 1-12, Nov 2020. <https://doi.org/10.1016/j.molliq.2020.113928>
- [19] R. Tayebee, A. H. Nasr, “Studying adsorption and detoxification of sulfur mustard chemical warfare onto ZnO nanostructures”, Journal of Molecular Liquids, vol. 319, pp. 1-10, 2020. <https://doi.org/10.1016/j.molliq.2020.114357>
- [20] R. M. A. Putri, T. Yuanita, M. Roelianto, “Daya Anti Bakteri Ekstrak Kulit Nanas (*Ananas comosus*) terhadap Pertumbuhan Bakteri *Enterococcus Faecalis*, Conservative Dentistry Journal, vol. 6, no. 2, pp. 61-65, 2016. <https://doi.org/10.20473/cdj.v6i2.2016.61-65>
- [21] N. A. Mirgane, V. S. Shivankar, S. B. Kotwal, G. C. Wadhawa, M. C. Sonawale, “Waste Pericarp of *Ananas comosus* in Green Synthesis Zinc Oxide Nanoparticles and their Application in Wastewater Treatment”, Materials Today: Proceedings, vol. 37, no. 2, pp. 886-889, 2020. <https://doi.org/10.1016/j.matpr.2020.06.045>
- [22] R. Santika, L. Rohmawati, “Analysis of Crystalline Phase and Functional Groups of ZnO from Pineapple Peel Extract, Indonesian Physical Review, vol. 5, no. 3, pp. 148-156, 2022. <https://doi.org/10.29303/ipr.v5i3.160>
- [23] D. Smazna, S. Shree, O. Polonskyi, S. Lamaka, M. Baum, M. Zheludkevich, F. Faupel, R. Adelung, Y. K. Mishra, “Mutual Interplay of ZnO Micro- and Nanowires and Methylene Blue During Cyclic Photocatalysis Process”, Journal of Environmental Chemical Engineering, vol. 7, no. 2, pp. 1-11, 2019. <https://doi.org/10.1016/j.jece.2019.103016>
- [24] H. Sadiq, F. Sher, S. Sehar, E. C. Lima, S. Zhang, H. M. N. Iqbal, F. Zafar, M. Nuhanovic, “Green Synthesis of ZnO Nanoparticles from *Syzygium Cumini* Leaves Extract with Robust Photocatalysis Applications”, Journal of Molecular Liquids, vol. 335, pp. 1-9, 2021. <https://doi.org/10.1016/j.molliq.2021.116567>
- [25] R. A. R. Ahmad, Z. Harun, M. H. D. Othman, H. Basri, M. Z. Yunos, A. Ahmad, S. H. M. Akhair, A. Q. A. Rashid, F. H. Azhar, A. R. Ainuddin, “Biosynthesis of zinc oxide nanoparticles by using fruits extracts of *Ananas comosus* and its antibacterial activity”, Malaysian Journal of Fundamental and Applied Sciences, vol. 15, no. 2, pp. 268-273, 2019. <https://doi.org/10.11131/mjfas.v15n2.1217>
- [26] M. Sari, Y. Rati, T. M. Linda, Y. Hamzah, A. S. Rini, “Biosynthesis of ZnO Micro-Nanoflower with *Ananas comosus* Peel Extract”, Journal of Aceh Physics Society, vol. 10, no. 4, pp. 84-87, 2021. <https://doi.org/10.24815/jacps.v10i4.18951>
- [27] P. C. Nagajyothi, S. J. Cha, I. J. Yang, T. V. M. Sreekanth, K. J. Kim, H. M. Shin, “Antioxidant and Anti-Inflammatory Activities of Zinc Oxide Nanoparticles Synthesized using *Polygala tenuifolia* Root Extract”, Journal of Photochemistry and Photobiology B: Biology, vol. 146, pp. 10-17, May 2015. <https://doi.org/10.1016/j.jphotobiol.2015.02.008>
- [28] S. Jurablu, M. Farahmandjou, T. P. Firoozabadi, “Sol-Gel Synthesis of Zinc Oxide (ZnO) Nanoparticles: Study of Structural and Optical Properties”, Journal of Sciences, Islamic Republic of Iran, vol. 26, no. 3, pp. 281-285, 2015.
- [29] H. H. Basri, R. A. Talib, R. Sukor, S. H. Othman, H. Ariffin, “Effect of Synthesis Temperature on the Size of ZnO Nanoparticles Derived from Pineapple Peel Extract and Antibacterial Activity of ZnO-Starch Nanocomposite Films”, Nanomaterials, vol. 10, no. 6, pp. 1-15, Jun 2020. <https://doi.org/10.3390/nano10061061>
- [30] I. S. Saputra, S. Suhartati, Y. Yulizar, Sudirman, “Green Synthesis Nanopartikel ZnO Menggunakan Media Ekstrak Daun Tin (*Ficus carica* Linn)”, Jurnal Kimia dan Kemasan, vol. 42, no. 1, pp. 1-6, Apr 2020. <http://dx.doi.org/10.24817/jkk.v42i1.5501>
- [31] M. M. Chikkanna, S. E. Neelagund, K. K. Rajashekarappa, “Green Synthesis of Zinc Oxide Nanoparticles (ZnO NPs) and their Biological Activity”, SN Applied Sciences, vol. 1, no. 117, pp. 1-10, Dec 2019. <https://doi.org/10.1007/S42452-018-0095-7>
- [32] A. Falihi, N.M. Ahmed, M. Rashid, “Green Synthesis of Zinc Oxide Nanoparticles by Fresh and Dry Alhagi Plant”,



- Materials Today: Proceedings., 49 (8), 3624–3629, 2022. <https://doi.org/10.1016/j.matpr.2021.08.201>
- [33] S. M. T. H. Moghaddas, B. Elahi, V. Javanbakht, “Biosynthesis of Pure Zinc Oxide Nanoparticles using Quince Seed Mucilage for Photocatalytic Dye Degradation”, *J. Alloys Compd.*, 821, 1-9, 2020. <https://doi.org/10.1016/j.jallcom.2019.153519>
- [34] A. Bagabas, A. Alshammari, M. F. A. Aboud, H. Kosslick, “Room-temperature synthesis of zinc oxide nanoparticles in different media and their application in cyanide photodegradation”, *Nanoscale Research Letters*, vol. 8, pp. 1-8, 2013. <https://doi.org/10.1186/1556-276x-8-516>
- [35] M. Bouloudenine, H. Laala-Bouali, K. Djeddou, M. Bououdina, N. Grara, “Chemical Route Manufactured ZnO Nanoparticles and their Biological Accumulation”, *Journal of Inorganic and Organometallic Polymers and Materials*, vol. 32, no. 6, pp. 1966–1974, Feb 2022. <http://dx.doi.org/10.1007/s10904-022-02240-0>
- [36] M. Kaur, V. Kumar, P. Kaur, R. Sharma, “Effect of Synthesis Methods on Dielectric Performance of ZnO Nanoparticles”. *Materials Technology*, vol. 37, no. 9, pp. 1156–1167, Jun 2022. <https://doi.org/10.1080/10667857.2021.1926777>
- [37] E. F. Barbosa, J. A. Coelho, E. R. Spada, D. R. B. Amorim, L. M. C. Souza, N. J. A. Cordeiro, H. D. Santana, J. L. Duarte, J. B. Floriano, W. H. Schreiner, A. G. Macedo, R. M. Faria, P. C. Rodrigues, “ZnO Nanoparticles, Nanorods, Hexagonal Plates and Nanosheets Produced by Polyol Route and the Effect of Surface Passivation by Acetate Molecules on Optical Properties”, *Journal of Electronic Materials*, vol. 48, no. 10, pp. 6437–6445, Jul 2019. <https://doi.org/10.1007/s11664-019-07446-6>
- [38] P. Lad, V. Pathak, A. B. Thakkar, P. Thakor, M. P. Deshpande, S. Pandya, “ZnO Nanoparticles Synthesized by Precipitation Method for Solar-Driven Photodegradation of Methylene Blue Dye and its Potential as an Anticancer Agent”, *Brazilian Journal of Physics*, vol. 53, no. 63, pp. 1-14, March 2023. <https://doi.org/10.1007/s13538-023-01278-w>
- [39] T. M. Abdelghany, A. M. H. A. Rajhi, R. Yahya, M. M. Bakri, M. A. A. Abboud, R. Yahya, H. Qanash, A. S. Bazaid, S. S. Salem, “Phytofabrication of Zinc Oxide Nanoparticles with Advanced Characterization and its Antioxidant, Anticancer, and Antimicrobial Activity Against Pathogenic Microorganisms”, *Biomass Conversion and Biorefinery*, vol. 13, no. 1, pp. 417–430, Oct 2023. <https://doi.org/10.1007/s13399-022-03412-1>
- [40] F. Ascencio, C. R. Damián, R. Escudero, “Clear antiferromagnetism induced by vacancies in ZnO nanoparticles synthesized by alkali salt method”, *Journal of Nanoparticle Research*, vol. 24, no. 91, pp. 1-12, Apr 2022. <https://doi.org/10.1007/s11051-022-05473-9>
- [41] A. Manohar, J. Parka, D. D. Geletaa, C. Krishnamoorthic, R. Thangamb, H. Kanga, J. Lee, “Synthesis and Characterization of ZnO Nanoparticles for Photocatalysis, Antibacterial and Cytotoxicity in Kidney Cancer (A498) Cell Lines” *Journal of Alloys and Compounds*, vol. 874, pp. 1-10, Sept 2022. <https://doi.org/10.1016/j.jallcom.2021.159868>
- [42] A. Saka, J. L. Tesfaye, L. Gudata, R. Shanmugam, L. P. Dwarampudi, N. Nagaprasad, R. Krishnaraj, S. Rajeshkumar, “Synthesis, Characterization, and Antibacterial Activity of ZnO Nanoparticles from Fresh Leaf Extracts of Apocynaceae, *Carissa spinarum* L. (Hagamsa)”. *Journal of Nanomaterials*, vol. 2022, pp. 1-6, 2022. <https://doi.org/10.1155/2022/6230298>
- [43] U. Wijesinghe, G. Thiripuranathar, H. Iqbal, F. Mena, “Biomimetic Synthesis, Characterization, and Evaluation of Fluorescence Resonance Energy Transfer, Photoluminescence, and Photocatalytic Activity of Zinc Oxide Nanoparticles”, *Sustainability*, vol. 13, no. 4, pp. 1–22, 2021. <https://doi.org/10.3390/su13042004>
- [44] G. A. Alharshan, A. M. Aoraia, M. A. M. Uosif, I. M. Sharaf, E. R. Shaaban, M. Saad, H. A. Mohiy, M. M. Elsenety, “Optical Band Gap Tuning, DFT Understandings, and Photocatalysis Performance of ZnO Nanoparticle-Doped Fe Compounds”, *Materials*, vol. 16, no. 7, pp. 1-12, March 2023. <http://dx.doi.org/10.3390/ma16072676>
- [45] R. Vinayagam, S. Pai, G. Murugesan, T. Varadavenkatesan, R. Selvaraj, “Synthesis of Photocatalytic Zinc Oxide Nanoflowers using *Peltophorum Pterocarpum* Pod Extract and their Characterization”, *Applied. Nanoscience*, vol. 13, pp. 847–857, Jun 2023. <https://doi.org/10.1007/s13204-021-01919-z>
- [46] M. R. A. Kumar, C. R. Ravikumar, H. P. Nagaswarupa, B. Purshotam, B. A. Gonfa, H. C. A. Murthy, F. K. Sabir, S. Tadesse, “Evaluation of Bi-Functional Applications of ZnO Nanoparticles Prepared by Green and Chemical Methods”, *Journal of Environmental Chemical Engineering*, vol. 7, no. 6, 2019. <https://doi.org/10.1016/j.jece.2019.103468>